Realization and Use of an IR Camera for Laboratory and On-field Electroluminescence Inspections of Silicon Photovoltaic Modules

Realization and Use of an IR Camera for Laboratory and On-field Electroluminescence Inspections of Silicon Photovoltaic Modules

Alessandro Ciocia[1], Alessio Carullo[2], Paolo Di Leo[1], Gabriele Malgaroli[1], and Filippo Spertino[1]

[1]Energy Department, [2]Electronics and Telecommunications Department, Politecnico di Torino, Torino, Corso Duca degli Abruzzi 24, 10129, Italy, alessandro.ciocia@polito.it

***Abstract* — Electroluminescence (EL) is a non-destructive technique, which detects the most common defects in Photovoltaic (PV) modules. High resolution EL images are generally obtained by infrared-sensitive cameras equipped with different semiconductors (indium gallium arsenide or silicon sensors). In the present work, a procedure is proposed to build and set up a high resolution EL camera for crystalline Si modules, equipped with a low-cost Si sensor. It can be used to perform EL test both indoor (lab) and outdoor (on-field). Experimental results from real PV plant highlight the combined use of *I-V* curves and EL images, for determining the amount of power losses and their causes.**

***Index Terms* — photovoltaic, maintenance, faults, electroluminescence, current-voltage characteristic.**

I. Introduction

During 2018, PhotoVoltaic (PV) has been the most installed technology in the word, with a new capacity of ≈100 GW [1]. The large diffusion of PV power plants, occurred mainly in the last decades, requires even more accurate and easily-use diagnostics methods to verify the state of health of the PV modules (degradation [2][3]) and guarantee a consequent high performance, long life and return of investment.

The most important test used to check the state of a PV generator consists of the determination of its current-voltage (*I-V*) characteristic curve by dynamic methods [4]. As well known in literature, it should be performed with adequate and calibrated measurement systems [5], using capacitive or electronic loads. Thanks to the capacitive load [6], the scan of the entire *I-V* curve can be easily performed at module, string and array level up to several hundreds of kilowatts. It has the following purposes: to measure the actual electric parameters of the PV generators (such as the performance) and compare them with the values indicated by the manufacturer. *I-V* characterization is also widely used to evaluate the PV performance evolution over time, due to the physiological decay of the module materials and quantify losses due to extraordinary/unexpected events, such as special atmospheric events (e.g. lightning and violent hailstorms) or damage during maintenance (e.g. walkway on the modules) [7]. The only limitation of this technique is that it cannot easily provide information about the causes of the electric parameters deviation.

In order to define the causes of underperformance, the conventional methods were the photoconductivity decay, the spectroscopic Laser Beam Induced Current (LBIC), and the Electron Beam Induced Current (EBIC) methods [8]. LBIC is based on the measurement of the local short circuit current of the cell, produced through laser excitation. The solar cell is contacted and locally irradiated by a laser; measurement is stored, and the laser is moved to another point of the cell. The result is a spatial map of the current produced by the cell, showing regions with lower production. A common problem with LBIC, which limits its industrial applicability, is the long measurement time, due to a combination of long motion and measurement time [9].

In recent years, thermography and Electroluminescence (EL) tests are even more used to define the modules affected by failures. The thermographic inspection allows a fast localization of potential defects at cell and module level as well as the detection of possible electrical interconnection problems. An Infrared (IR) thermo-camera works as a video recording device (in the spectral range 7—14 μm), which produces a radiometric thermal image. The result is a spatial map of the temperatures of the modules, showing regions with cooler or hotter temperatures [10]. Well working cells exhibit near-uniform current density in reverse bias and heat load is well distributed across the module. On the contrary, defective cells manage the current flow through a small area of silicon, that cause a high temperature area (hot-spot) that can damage the cell within seconds. The inspections are carried out under normal operating conditions and do not require a system shut down [11].

Compared to thermography, EL offers a considerably improved image resolution and level of detail [12][13]. Thanks to EL, the typology of defects affecting the PV modules is defined, with accuracy and a low cost. The visual analysis of the IR images permits to justify the performance deviation with mechanical/chemical defects. Some researchers [14] are working to avoid the scan of the *I-V* curve: their purpose is to extract the information of the electrical parameters only from the EL test results. Nevertheless, the results are partial or limited to few

typologies of defects [15] and cannot provide accurate/complete electrical results. The two above defined techniques are complementary: the determination of the *I-V* curve allows a quantitative evaluation of performance of the PV module, while the EL gives a qualitative state of health of the devices.

A recent line of research is aimed at identifying malfunctions in the modules starting from the scanning of the *I-V* curve, by determining the parameters of the equivalent electric circuit. The variation of the parameters, such as the shunt and series resistances [16], are studied and validated by EL inspection results. The present paper is organized as follows: first, the EL test is described, with details about the principle of operation and a summary of the identifiable defects. Then, it is presented a procedure to build an accurate low-cost EL camera modifying a commercial CMOS camera. Finally, experimental results both in laboratory and on-field are shown, with related comment and conclusions.

II. DESCRIPTION OF ELECTROLUMINESCENCE TEST

A. Principle of operation of Electroluminescence test

The EL test requires the devices described as follows.

1) A camera can capture IR radiation from PV modules. In case of on-field inspection, the camera should be portable, especially in case of on-field inspections.

2) A variable power supply permits to apply the appropriate voltage and current to the PV generator for the luminescence emission under dark conditions. The setup depends on environmental conditions and generator specifications (details in Section IV).

3) A personal computer is equipped with a card reader unit to acquire EL images with a post processing software.

The EL test starts with the application of a forward bias to the PV generator, in a totally shaded condition (dark room in laboratory or on-field with irradiance G<50—100 W/m^2). The PV cells work like LEDs (Light Emitting Diodes), in which their semiconductor materials have emission spectra in the IR region of the electromagnetic spectrum (between about 400 and 700 nm) and not in the visible region. As shown in Fig.2, the luminescence signal from crystalline silicon ranges from about 950 nm to ≈1350 nm and the peak, corresponding to the band gap, is of 1150 nm. The emitted photons can be detected by a sensitive camera equipped with indium gallium arsenide (InGaAs) photodiodes, or silicon devices, i.e. silicon charge-coupled device (CCD) or CMOS. In case of InGaAs, the emission curve of crystalline silicon well matches the absorption curve of the InGaAS detector, with about 80% of quantum efficiency in correspondence of the emission peak (Fig.3).

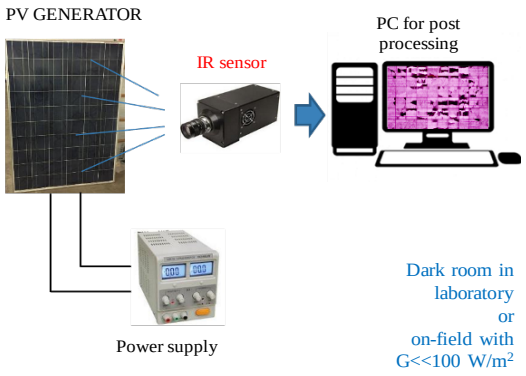

Fig. 1. Equipment necessary for the EL test.

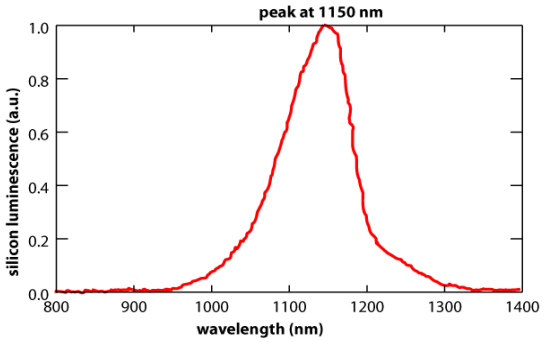

Fig. 2. The luminescence signal of silicon peaks at 1150 nm corresponding to the energy of the bandgap, from [17].

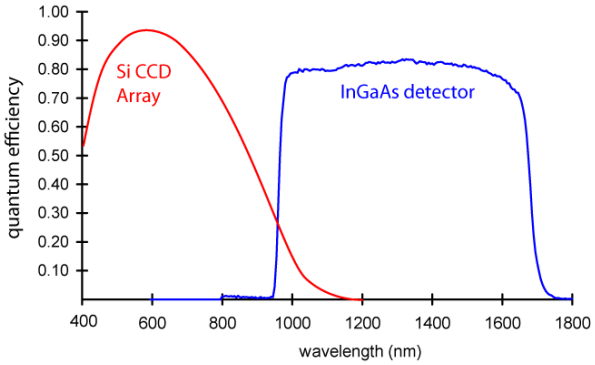

Fig. 3. Quantum efficiency of silicon CCD detectors and InGaAs photodiode array, from [18].

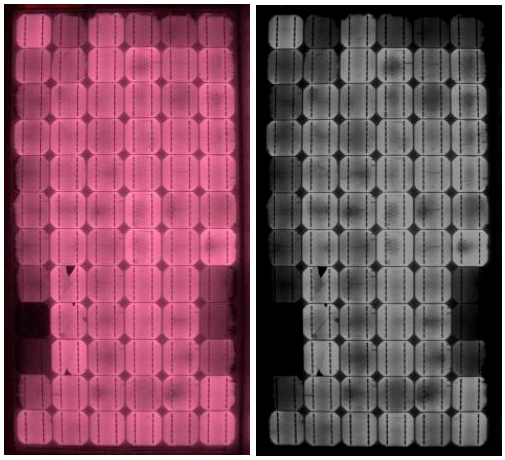

Fig. 4. EL image of a 72 m-Si cells module affected by PID, performed by the CCD camera used in the present work (left) and an InGaAs camera used in [20] (right).

InGaAs sensors guarantee high image resolution, but also high cost for the sensor (between thousands and tens thousands of euros). On the other hand, the CCD/CMOS sensor has a relatively poor response over the 1000—1200 nm region of interest, but its cost is negligible (it can be <<1000 €) [19].

For this reason, the use of CMOS camera is even more interesting, and researchers are working to exploit the best possible the poor response of the CMOS sensor.

The results can be very good: as shown in Fig.4. The image quality of an EL test carried out by the CMOS sensor used in the present work (left) is comparable with the one obtained by an InGaAS camera (right). No particular differences can be detected, also increasing the image size.

B. Defects identifiable by the Electroluminescence tests

The EL test permits to detect different types of defects and faults, that may occur during the whole life of the PV module, i.e. the manufacturing process, transportation, installation and maintenance. A description of the most important defects, detectable by EL, is listed below [20].

1) Micro-cracks can be generated during production, during transportation and on-field. The most common type of micro-cracks appears on-field during installation and operation, caused by human and environmental causes (e.g., thermal stress, hail, storm and lightning). Regarding human cause, the walkway on PV modules must be avoided during installation and maintenance. It can be performed by appropriate organization and design of the PV plant [7][21]. It is not trivial to determine in which phase of life the micro-cracks are produced, because in many cases the shape of the cracks is similar and energy losses are variable [22].

2) Broken cells: mechanical or thermal stresses can transform micro-cracks into broken cells (Fig.5α). Cracks involve the electrical isolation of cells portions, with a limitation in the current in the whole string of series-connected cells. Cracks are one of the main sources of power loss in the PV modules (Fig.5β).

3) Impurities are due to low quality production processes: an example is a no uniform temperature distribution during the firing of the electric connections, causing higher resistance areas (darker in Fig.5γ).

4) Potential Induced Degradation (PID) is a degradation of the *I-V* curve of the PV generator caused by a leakage currents towards the frame. High voltage with respect to ground and high temperature and humidity are the driving factors. The result is the electric isolation of some PV cells and high power loss at the module level. In

the bottom part of Fig.5δ, the two darker cells are PID affected, with the edges (close the frame) totally inactive and black.

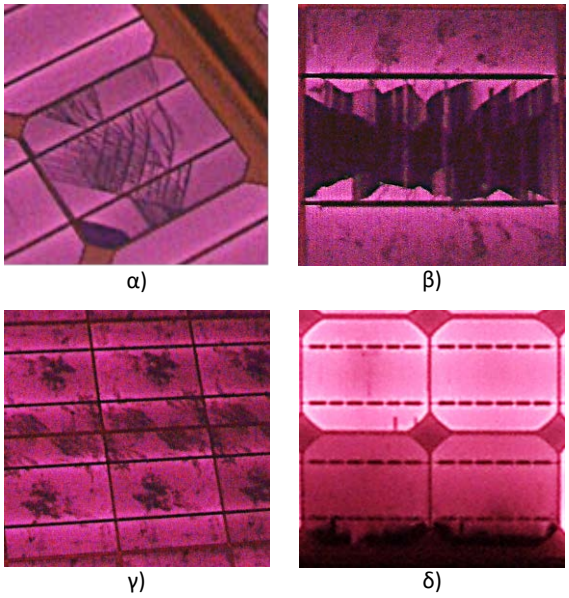

Fig. 5. Examples of defects in PV cells detectable by EL test.

III. CONSTRUCTION OF A CCD CAMERA AND POWER SUPPLY SELECTION FOR ON-FIELD ELECTROLUMINESCENCE

A. EL camera construction

In order to perform accurate EL test, it is possible to use commercial CMOS camera, after an appropriate modification. These devices are designed for acquiring visible light. Nevertheless, as abovementioned, the CMOS sensor has the capability of capturing also a part of IR and ultraviolet radiation. Thus, manufacturers use different filtering methods to block the radiation outside the visible range, otherwise the photographs would be characterized by incorrect colors and other issues. In particular, the sensors are generally protected by two filters for IR radiation:

1) The main filter consists of a glass placed directly above the sensor, which has the capability of removing almost all the IR radiation. With this filter, it is quite impossible to perform an acceptable EL test; it is necessary the opening of the camera and the removal of the filter.

2) The second filter is made up a coating inside the lens of the camera. This coating is much less effective of the main filter; thus, it is possible to perform the EL test with standard lenses, but with a much longer exposure time and some prescriptions described below.

In the present work, the internal IR filter of a CMOS camera is removed, and the lens is substituted with another allowing the IR radiation to pass. A commercial Digital Single-Lens Reflex (DSLR) camera, model D3200 from the manufacturer Nikon is modified [23]. The CMOS sensor size is 23.2 mm x 15.4 mm and it is characterized by a maximum resolution of 24.2 megapixels and a sensitivity range 100—6400 ISO [24]. This resolution permits to acquire small details of the solar cells (such as cracks and the consequent edges of broken cells), while a high ISO sensitivity value could be useful in case of low emission from the PV generators. The DSLR camera uses interchangeable lenses (model F-mount), which facilitates the use of specific lenses for IR radiation. The above-mentioned specifications can be used as a reference. Different camera models from the most important manufacturers are suitable for the EL purposes. In particular, an increment in the size of the sensor, with respect to the proposed one (i.e. the commercial size called “full frame” measures 24 mm x 36 mm), can even more improve the performance of the EL test, but also the costs. Regarding the ISO sensitivity, the setup of the maximum value is not recommended, because the resolution dramatically decreases if the sensor is forced to work at a too high ISO value. Fig. 6 summarizes the steps for the IR filter removal. First, external lens is removed from the camera (a). Then, screws and rubber grip are removed to open the camera and access the internal electronic board (b). After the removal of other screws and disconnection of boards cables, the enclosure of the filter is accessible (c). The IR filter (consisting of a colored glass positioned in contact with the sensor) can be removed (d) and the camera can be reassembled. Regarding the appropriate external lenses, in the present work, the modified D3200 camera is equipped with a lens designed to allow passing IR radiation especially from 900 to 1400 nm, with a fixed focal length (50mm) and with high focal aperture N=1.4 [25]. The

main issue related to the selected lens is the absence of automatic focus, which involves a continuous manual focus on the PV modules, when the distance between camera and PV generators varies.

In [26], the use of a substitutive internal filter is proposed, instead of the one removed from the camera, to stop radiation above 700—800 nm. The goal consists of avoiding interferences due to external sources of light, that are filtered. It can be useful in case of LED lights of public lighting (that cannot be switched off during the test) close to the modules. Nevertheless, other sources of light that can interfere are generally missing on-field, especially close to large PV plants, and in the present work the additional filter is not used. Obviously, if irradiance is present (G>50—100 W/m^2), the additional filter is useless: solar radiation includes infrared, and the test cannot be performed.

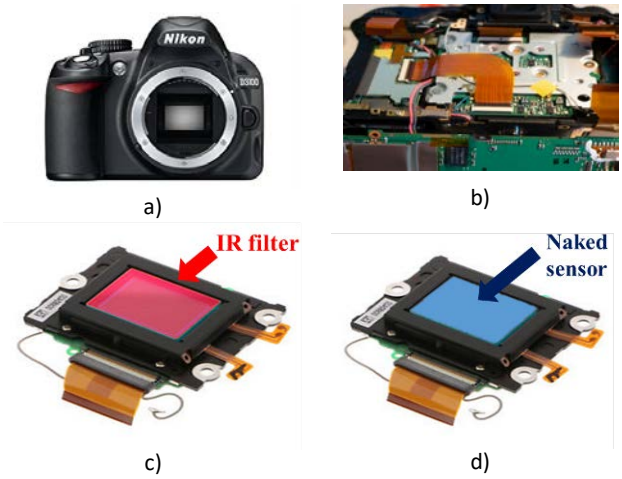

Fig. 6. Procedure for the filter removal in a commercial DSLR.

B. EL camera setup

Images are acquired with the EL camera and stored for post processing; nevertheless, some parameters shall be chosen also during the test. The setup of the camera varies as a function of the PV system and of the environmental conditions. As in traditional photography, the main parameters to setup for a correct image are the three used for camera selection: focal aperture, sensor sensitivity ISO, and exposition time. Due to the special conditions in which the photo is acquired (during night in front of the modules emitting a low IR light), the setup is the following. First, the maximum focal aperture is used; then, the sensor sensitivity is setup at a medium level (i.e. 800 ISO) and finally the exposure time is selected iteratively, starting from a value of ≈0.5 s. As a function of the camera and lens specifications, the time must be increased, as long as it is adequate to get a clear image (up to tens of seconds in the worst case).

C. Power supply selection

During EL tests, PV modules are forward biased: voltage is equal to the open circuit voltage of the generator at Standard Test Condition (STC, irradiance G=1000 W/m^2, cell temperature T_c=25°C and air mass AM=1.5) and the excitation current has to be in the range 50—100% of the short circuit current at STC [17]. Luminescence is proportional to the current; defective areas appear darker than working areas. According to [27], the variation of external excitation current in EL permits to investigate different defects: low current densities are used to study the material properties, while high current permits to test the properties of the electrical contacts. In order to properly size the power supply, its maximum current should be equal or higher the short circuit current of the PV generator.

The open circuit voltage V_{oc} (T) can be easily calculated by the formula depending on temperature:

$$V_{oc}(T)=V_{oc,STC}\cdot[1+\beta_V\cdot(T\text{-}25°C)] \qquad (1)$$

where $V_{oc,STC,}$ is the open-circuit voltage at STC and β_V (%/°C) is the thermal coefficient for voltage.

Obviously, the DC power supply has also to match the power required by the PV generator at the above-mentioned current and voltage levels. For example, a PV string is composed of 24 series-connected PV modules. Each PV module is characterized by a short-circuit current I_{sc}=8 A and an open-circuit voltage V_{oc}=36 V at STC. At STC, the power supply must provide 864 V and 8 A, corresponding to 6.912 kW. If the test is performed at a lower temperature (e.g. during a winter night) voltage could be much higher. With a module temperature of 0°C, and a typical value β_V=-0.33 %/°C for crystalline modules, the same PV string requires ≈935 V. As a conclusion, in

case of inspection of large plants, in which the disconnection of the single modules is too expensive, EL test of entire strings could require a DC power supply with voltage range up to 1000 V.

IV. LABORATORY AND ON-FIELD EXPERIMENTAL RESULTS

A. Electroluminescence in laboratory

The EL test can easily be performed in a dark room of a laboratory: external light sources are avoided and the camera can be mounted on a tripod to avoid a blurry image also in case of long exposure time. Fig. 7 shows a comparison between visual, EL and thermography inspections on a polycrystalline silicon module with a rated power of 228 W and composed of 60 cells. Electrical rated parameters are shown in Table I. Visual inspection and thermography were done on-field, but they did not show any defect; in particular, there are no hot spots. On the contrary, the EL test was performed in laboratory with the camera described in the previous section, and it shows that almost all the cells are broken or have cracks: only five cells out of sixty are not damaged.

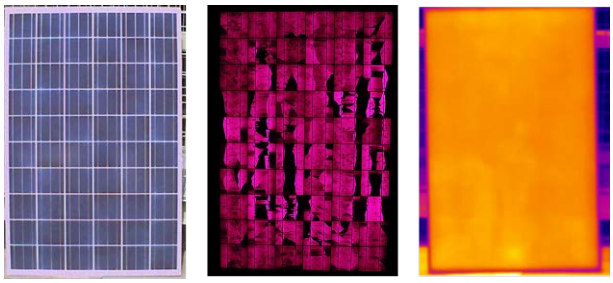

Fig. 7. A comparison between visual, EL and thermography inspections.

The breakage of cells was caused by the walkway on the modules due to the lack of walkways. The result is an underperformance of -33%, with respect to the datasheet. This deviation is calculated from the *I-V* curve characterization, whose results are summarized in Table II. The tests were performed at irradiance G≈700 W/m^2 with an air temperature of 14°C and cell temperature T_c≈34°C. All the *I-V* curve is defined, starting from short circuit to open circuit conditions, with special attention for the maximum power point.

TABLE I
RATED ELECTRIC PARAMETERS (@ STC)

V_{mpp}	29.93	V	η	14.2%	
I_{mpp}	7.65	A	I_{sc}	8.16	A
P_{mpp}	228	W	V_{oc}	36.20	V
Tolerance (P_{mpp})	±3%		***Fill Factor***	77.2%	

TABLE II
MEASURED ELECTRIC PARAMETERS (@ STC)

V_{mpp}	28.38	V	η	9.4%	
I_{mpp}	5.34	A	ΔV_{mpp}	-5.2%	A
P_{mpp}	152	W	ΔI_{mpp}	-30%	V
Deviation vs. Datasheet	-33%		***Fill Factor***	62,5%	

Experimental curve is then corrected to STC by the procedure defined in the Standards [28]. The obtained maximum power $P_{mpp}=V_{mpp}\cdot I_{mpp}$ is compared with the one declared in the datasheet of the module, and the deviation is quantified. The measurement uncertainties are defined in [22] and tests are repeated three times to guarantee repeatability. In the module under study, the power deviation is mainly due to a current drop ΔI_{mpp}=-30%, while the voltage loss is of secondary importance (ΔV_{mpp}≈-5%). As a consequence of both effects, the efficiency decreases from the datasheet value η=14.2% to 9.4% and the maximum power from 228 W to 152 W. As a result, the Fill Factor (FF) indicator, calculated to compare the quality of PV generators as $FF= P_{mpp}/(I_{sc}\cdot V_{oc})$ is much lower than the value declared by the manufacturer.

B. Electroluminescence on-field

The walkway on modules is again the cause of micro-cracks and broken cells in the roof-top plant, whose planimetry is shown in Fig. 8 (each color corresponds to a different string). Strings are mounted close to each other; thus, during installation and maintenance modules were damaged by workers. The result is a distribution of defects in all the PV arrays, with few modules excluded. Fig. 9 shows an overview of some modules analyzed by the EL camera. The test was performed during night without the modules disconnection. Each string was forward biased one after the other, and the operator moved on the plant with the portable camera.

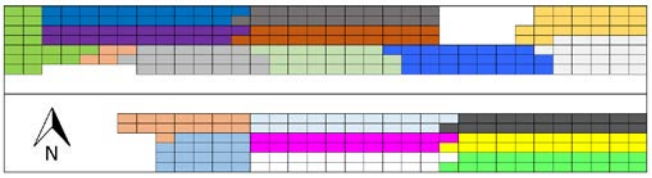

Fig. 8. Planimetry of the roof-mounted PV plant under study.

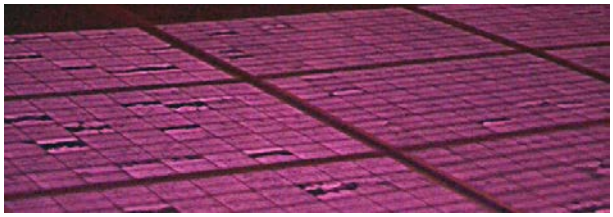

Fig. 9. On-field EL overview of roof-mounted PV modules.

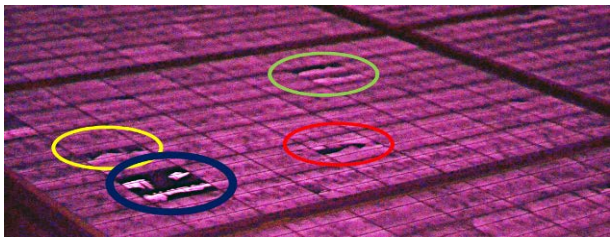

Fig. 10. On-field EL image of a PV module with broken cells.

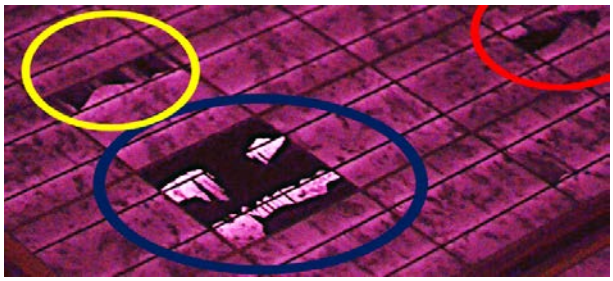

Fig. 11. EL detail of defective cells in the modules of Fig. 9.

In case of defects detection (Fig. 10), the module is analyzed more closely and details about failures are stored with high resolution (Fig. 11). The *I-V* curve characterization shows high power deviations for all the 18 strings composing the plants, with values from -12% up to -20%. The *I*-V and power-voltage (P-V) curves of one string are shown in Fig.12. The shape of *I-V* curve is not smooth near the maximum power point due to broken cells. Moreover, the current starts decreasing from short circuit condition, due to a decreased shunt resistance with respect to a well working module. Thus, to recover the energy production of the plant, the replacement of the modules will start with those affected by the highest number of defects in those strings with the highest power losses.

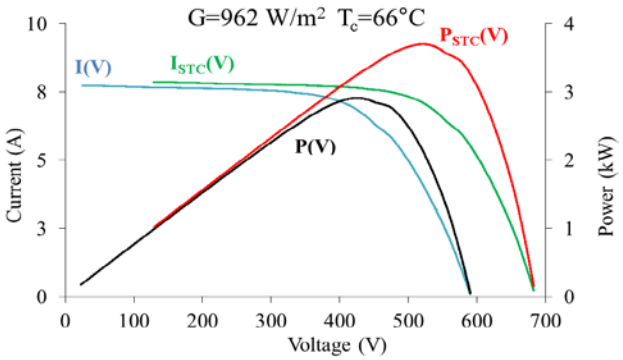

Fig. 12. *I-V* and *P-V* measured curves and their shift to STC.

IV. CONCLUSIONS

The *I-V* characterization of PV generators and the EL test are two complementary diagnostics techniques. The determination of the *I-V* curve allows a quantitative evaluation of the PV module performance, while the EL gives a qualitative state of health, with details about the causes of the failures. This property makes the EL a better technique than thermography, which in many cases can only localize the defects, if they generate no uniform temperature, and not define their causes. To perform a cheap and easy EL test, a procedure is provided to build, setup and use an EL camera, based on the modification of a commercial CMOS camera. The results are comparable with those of expensive InGaAs cameras. This equipment can be used in laboratory and on-field to identify failures in large plants. After the rapid scan of the *I-V* curve of entire arrays, the disconnection of each module and its measurement is not required. Thanks to EL, the modules with more failures from the worst strings can be selected to be replaced.

ACKNOWLEDGMENT

The authors want to thank Andrea Cerrato and the Staff of the company Cms Italia s.r.l. working in the thermomechanical sector and in the design and production of industrial electronic equipment. They collaborated offering spaces and part of the instrumentation to perform the experimental activity described in this paper.

REFERENCES

[1] Renewables Energy Policy Network, Renewables 2018 Global Status Report, 2018. [Online]. Available: http://www.ren21.net/status-of-renewables/global-status-report/

[2] A. Carullo, A. Vallan, A. Ciocia and F. Spertino, “Degradation tests and characterization procedures of Photovoltaic modules exposed to outdoor conditions.” *in 22nd IMEKO TC-4 International Symposium on Measurement in Research and Industry*, 2015, Prague, pp. 1-6.

[3] A. Carullo, A. Castellana, A. Vallan, A. Ciocia and F. Spertino, “Experimental assessment of degradation rate in photovoltaic modules”, in *21st IMEKO TC-4 International Symposium and 19th International Workshop on ADC Modelling and Testing*, 2016, Budapest, pp. 158-163

[4] F. Spertino, J. Sumaili, H. Andrei and G. Chicco, "PV Module Parameter Characterization From the Transient Charge of an External Capacitor," *IEEE Journal of Photovoltaics*, vol. 3, no. 4, pp. 1325-1333, 2013.

[5] A. Carullo, A. Castellana, A. Vallan, A. Ciocia and F. Spertino, “Uncertainty issues in the experimental assessment of degradation rate of power ratings in photovoltaic modules,” *Measurement*, vol 111, pp 432-440, 2017.

[6] F. Spertino, J. Ahmad, A. Ciocia, P. Di Leo, Ali F. Murtaza and M. Chiaberge, “Capacitor charging method for I–V curve tracer and MPPT in photovoltaic systems,” *Solar Energy*, vol 119, pp. 461-473, 2015.

[7] F. Spertino, J. Ahmad, A. Ciocia and P. Di Leo, “Techniques and Experimental Results for Performance Analysis of Photovoltaic Modules Installed in Buildings,” *Energy Procedia*, vol 111, pp. 944-953, 2017.

[8] T. Fuyuki and A. Kitiyanan, “Photographic diagnosis of crystalline silicon solar cells utilizing electroluminescence,” *Appl. Phys. A*, vol. 96, no. 1, pp. 189–196, 2009

[9] R. M. Geisthardt and J. R. Sites, "Nonuniformity Characterization of CdTe Solar Cells Using LBIC," *IEEE Journal of Photovoltaics*, vol. 4, no. 4, pp. 1114-1118, 2014.

[10] G. Schirripa Spagnolo, P. Del Vecchio, G. Makary, D. Papalillo and A. Martocchia, "A review of IR thermography applied to PV systems," i*n 11th International Conference on Environment and Electrical Engineering*, 2012, pp. 879-884, Venice.

[11] A. K. V. de Oliveira, M. Aghaei, U. E. Madukanya, L. Nascimento and R. Rüther, "Aerial Infrared Thermography of a Utility-Scale PV Plant After a Meteorological Tsunami in Brazil," *in IEEE 7th World Conference on Photovoltaic Energy Conversion (WCPEC) (A Joint Conference of IEEE PVSC, PVSEC & EU PVSEC)*, 2018, pp. 0684-0689, Waikoloa Village, HI.

[12] International Energy Agency, Review on Infrared and Electroluminescence Imaging for PV Field Applications, Report IEA-PVPS T13-10:2018, 2018. [Online]. Available: http://www.iea-pvps.org/index.php?id=371&eID=dam_frontend_push&docID=4318

[13] S. Koch, T. Weber, C. Sobottka, A. Fladung, P. Clemens, J. Berghold, “Outdoor Electroluminescence Imaging of Crystalline Photovoltaic Modules: Comparative Study between Manual Ground-Level Inspections and Drone-Based Aerial Surveys”, *in Proc. Of 32nd European Photovoltaic Solar Energy Conference and Exhibition*, pp. 1736-1740, 2016.

[14] C. A. Rodríguez Castañeda, S. Chattopadhyay, J. Oh, S. Tatapudi, G. TamizhMani and H. Hu, "Field Inspection of PV Modules: Quantitative Determination of Performance Loss due to Cell Cracks Using EL Images," in *IEEE 44th Photovoltaic Specialist Conference (PVSC)*, 2017, pp. 1858-1862, Washington, DC.

[15] K. G. Bedrich et al., "Quantitative Electroluminescence Imaging Analysis for Performance Estimation of PID-Influenced PV Modules," *IEEE Journal of Photovoltaics*, vol. 8, no. 5, pp. 1281-1288, 2018.

[16] D.M. Fébba, R.M. Rubinger, A.F. Oliveira, E.C. Bortoni, “Impacts of temperature and irradiance on polycrystalline silicon solar cells parameters,” *Solar Energy*, vol. 174, , pp. 628-639, 2018

[17] T. Fuyuki, Kondo, H., Yamazaki, T., Takahashi, Y., and Uraoka, Y., “Photographic surveying of minority carrier diffusion length in polycrystalline silicon solar cells by electroluminescence”, *Applied Physics Letters*, vol. 86, 2005.

[18] Photovoltaic Education Network, 2019. [Online]. Available: https://www.pveducation.org/pvcdrom.

[19] T. Weber, A. Albert, M. Roericht, S. Krauter, and P. Grunow, “Electroluminescence investigation on thin film modules,” in *26th European Photovoltaic Solar Energy Conference and Exhibition*, 2011.

[20] F. Spertino, A. Ciocia, P. Di Leo, R. Tommasini and I. Berardone, M. Corrado, A. Infuso, M. Paggi, “A power and energy procedure in operating photovoltaic systems to quantify the losses according to the causes,” *Solar Energy*, vol. 118, pp. 313-326, 2015

[21] International Energy Agency, Performance and Reliability of Photovoltaic Systems, Review of Failures of Photovoltaic Modules, Report, IEA-PVPS Task 13, 2014. [Online]. Available: http://iea-pvps.org/fileadmin/dam/intranet/ExCo/IEA-PVPS_T13-01_2014_Review_of_Failures_of_Photovoltaic_Modules_Final.pdf

[22] F. Spertino, A. Ciocia, F. Corona, P. Di Leo and F. Papandrea, "An experimental procedure to check the performance degradation on-site in grid-connected photovoltaic systems," *in IEEE 40th Photovoltaic Specialist Conference (PVSC)*, pp. 2600-2604, 2014 Denver.

[23] Wikipedia, 2019. [Online]. Available: https://en.wikipedia.org/wiki/Nikon_D3200.

[24] ISO Standard, Photography -- Colour negative films for still photography -- Determination of ISO speed, ISO 5800:1987

[25] ISO Standard, Photography—Apertures and related properties pertaining to photographic lenses, ISO 517:2008

[26] K. Mertens, Th. Stegemann, and T. Stöppel, “LowCost EL: Erstellung von Elektrolumineszenzbildern mit einer modifizierten StandardSpiegelreflexkamera,” in *27th Symposium Photovoltaische Solarenergie*, pp 214-219, Staffelstein, 2012

[27] R. Ebner, B. Kubicek and G. Ujvari, ”Non-destructive techniques for quality control of PV modules: infrared thermography, electro- and photoluminescence imaging”, *in 39th Annual Conference of the IEEE Industrial Electronics Society*, pp. 8104-8109, 2013.

[28] IEC 60891:2009-12, Photovoltaic devices - Procedures for temperature and irradiance corrections to measured I-V characteristics